Bat3 deficiency accelerates the degradation of Hsp70-2/HspA2 during spermatogenesis

Toru Sasaki,[1] Edyta Marcon,[4] Tracy McQuire,[1] Yoichi Arai,[5] Peter B. Moens,[4] and Hitoshi Okada[1,2,3]

[1]The Campbell Family Institute for Breast Cancer Research, [2]Division of Signaling Biology, Ontario Cancer Institute, University Health Network, and
[3]Department of Medical Biophysics, University of Toronto, Toronto, Ontario M5G 2C1, Canada
[4]Department of Biology, York University, Toronto, Ontario M3J 1P3, Canada
[5]Department of Urology, Tohoku University, School of Medicine, Aoba-ku, Sendai 980-8574, Japan

Meiosis is critical for sexual reproduction. During meiosis, the dynamics and integrity of homologous chromosomes are tightly regulated. The genetic and molecular mechanisms governing these processes in vivo, however, remain largely unknown. In this study, we demonstrate that *Bat3/Scythe* is essential for survival and maintenance of male germ cells (GCs). Targeted inactivation of *Bat3/Scythe* in mice results in widespread apoptosis of meiotic male GCs and complete male infertility. Pachytene spermatocytes exhibit abnormal assembly and disassembly of synaptonemal complexes as demonstrated by abnormal SYCP3 staining and sustained γ-H2AX and Rad51/replication protein A foci. Further investigation revealed that a testis-specific protein, Hsp70-2/HspA2, is absent in *Bat3*-deficient male GCs at any stage of spermatogenesis; however, Hsp70-2 transcripts are expressed at normal levels. We found that *Bat3* deficiency induces polyubiquitylation and subsequent degradation of Hsp70-2. Inhibition of proteasomal degradation restores Hsp70-2 protein levels. Our findings identify Bat3 as a critical regulator of Hsp70-2 in spermatogenesis, thereby providing a possible molecular target in idiopathic male infertility.

Introduction

Meiosis is a fundamental process for genetic exchange between maternal and paternal genomes in all eukaryotes. During prophase of the first meiotic division, homologous chromosomes undergo synapsis, genetic exchange, and gene conversion. Once paired, homologous chromosomes are connected by the synaptonemal complex (SC), a tripartite multiprotein structure. The SC consists of the central element, axial/lateral elements, and transverse filaments (Fawcett, 1956; Moses, 1956, 1969; Zickler and Kleckner, 1999). Formation of the fully synapsed autosomal SCs and the partially synapsed XY pair are essential for successful completion of DNA repair and recombination processes and subsequent desynapsis (Moens, 1994). Although the function and regulation of SC proteins are not fully understood, recent genome-wide screens and genetic studies have identified novel SC components (Wang et al., 2001; Maratou et al., 2004; Toure et al., 2005), including SYCE1, CESC1, and TEX12 (Costa et al., 2005; Hamer et al., 2006). These discoveries, combined with mouse genetics, have provided in-depth insight into the regulation of meiosis (Bolcun-Filas et al., 2007; Costa and Cooke, 2007).

Hsp70-2, another SC-interacting protein, is expressed exclusively in male germ cells (GCs) at specific stages of differentiation. Hsp70-2 is not expressed in spermatogonia but becomes detectable at leptotene and zygotene. Hsp70-2 is expressed highly in pachytene spermatocytes, where it has been found to associate with the lateral element of the SC (Allen et al., 1996). Consistent with this expression pattern, sperm development in *Hsp70-2*–deficient mice arrests in meiotic prophase I, and the majority of late pachytene spermatocytes are eliminated by apoptosis, resulting in complete male infertility (Dix et al., 1996). Recently, Hsp70-2 was reported to act as a chaperone of transition proteins TP1 and TP2 in spermatids (Govin et al., 2006).

Bat3 (also called *Scyth*; Thress et al., 1998) has been reported to regulate apoptosis in a variety of settings (Thress et al., 1998, 1999a,b; Desmots et al., 2005). Certain domains in Bat3

Correspondence to Hitoshi Okada: hokada@uhnres.utoronto.ca

Abbreviations used in this paper: BAG, Bcl-2–associated athanogene; FSH, follicle-stimulating hormone; GC, germ cell; KD, knockdown; LH, lutenizing hormone; poly-Ub, polyubiquitylation; RPA, replication protein A; SC, synaptonemal complex.

The online version of this article contains supplemental material.

The Rockefeller University Press $30.00
J. Cell Biol. Vol. 182 No. 3 449–458
www.jcb.org/cgi/doi/10.1083/jcb.200802113

also appear in the Bcl-2-associated athanogene (BAG) family of proteins that regulate Hsp70 function. Thus, Bat3 may be important for the folding and activity of apoptotic signaling molecules (Thress et al., 2001). Recently, p53 and apoptosis-inducing factor have been identified as Bat3 targets after DNA damage (Sasaki et al., 2007) and ER stress (Desmots et al., 2007), respectively. In addition, Bat3 has been shown to act as a ligand of a natural killer cell receptor (Pogge von Strandmann et al., 2007), suggesting that Bat3 may mediate signals from damaged cells to the immune system. However, although Bat3 is predominantly expressed in adult testes (Wang and Liew, 1994), the role of Bat3 in male GC development remains unknown.

In this study, we investigated male GC development in *Bat3*-deficient mice and found that most *Bat3*-deficient male GCs die of apoptosis at meiotic prophase I. Interestingly, the testis-specific Hsp70-2 protein was undetectable in *Bat3*-deficient cells even though Hsp70-2 transcript levels were normal. We found that *Bat3* inactivation induced polyubiquitylation (poly-Ub) and subsequent degradation of Hsp70-2. Additional inactivation of proteasome activity restored Hsp70-2 protein levels. We conclude that Bat3 functions as a critical regulator of Hsp70-2 in spermatogenesis.

Results and discussion

We detected high levels of Bat3 mRNA in adult testes (Fig. 1 A), which is consistent with a previous study (Wang and Liew, 1994). Male but not female $Bat3^{-/-}$ mice were completely infertile. We observed that $Bat3^{-/-}$ testes at postnatal day 120 (P120) were significantly smaller (Fig. 1 B). The mean weight of $Bat3^{-/-}$ testes (40.0 ± 7.0 µg; $n = 8$) was one third of the weight of $Bat3^{+/+}$ (125.0 ± 1.0 µg; $n = 8$) and $Bat3^{+/-}$ (115.0 ± 7.0 µg; $n = 8$) testes (Fig. 1 C). In contrast, no significant differences were observed in the size and weight of the epididymis for all three genotypes ($Bat3^{+/+}$, 25.0 ± 2.0 µg; $Bat3^{+/-}$, 24.0 ± 7.0 µg; $Bat3^{-/-}$, 23.0 ± 1.0 µg; $n = 8$; Fig. 1 D). In addition, serum levels of follicle-stimulating hormone (FSH), lutenizing hormone (LH), and testosterone were not significantly different between $Bat3^{+/+}$ and $Bat3^{-/-}$ mice (Table S1, available at http://www.jcb.org/cgi/content/full/jcb.200802113/DC1). These data indicate that the observed phenotypes are caused by intrinsic GC defects.

Histological analysis of testes from $Bat3^{+/+}$ and $Bat3^{-/-}$ mice revealed no significant differences at P7 (Fig. 1, E and I) and P14 (Fig. 1, F and J) when GCs have not yet developed beyond spermatogonia. Thus, mitotic proliferation of spermatogonia progenitors appears to proceed normally. Defects became obvious at P42 when $Bat3^{-/-}$ testes displayed very few late pachytene spermatocytes (Fig. 1, G and K). At P140, $Bat3^{-/-}$ testes contained significantly fewer spermatocytes and no spermatids or spermatozoa in most seminiferous tubules (Fig. 1, H and L). Consistent with these observations, sections of $Bat3^{-/-}$ epididymides revealed no spermatozoa at P140 (Fig. 1, M and N).

To further elucidate the defective stage of spermatogenesis in $Bat3^{-/-}$ mice, we investigated the transcript levels of GC-specific differentiation markers (Fig. 1 O). No differences in the expression of Plzf (a marker for germ stem cell and spermatogonial differentiation; Buaas et al., 2004) and Dazl (a spermatogonia-specific marker; Schrans-Stassen et al., 2001) were observed between $Bat3^{+/+}$ and $Bat3^{-/-}$ testes, suggesting that Bat3 is not essential for the production of spermatogonia. Similarly, phosphoglycerate kinase-2 (a spermatocyte-specific marker; Boer et al., 1987) was expressed normally in the $Bat3^{-/-}$ background. In contrast, protamine 1, the mature haploid GC-specific marker expressed in postmeiotic GCs (Kleene et al., 1984), was undetectable in $Bat3^{-/-}$ testes, indicating a severe defect in GC differentiation beyond meiosis. We also found that GATA-1, a marker of Sertoli cells, was expressed normally in $Bat3^{-/-}$ testes.

We next investigated whether *Bat3* deficiency induces apoptosis in male GCs at various developmental stages. Apoptotic cells were rarely detected at P7 (Fig. 1, P and Q). In contrast, the number of apoptotic cells increased significantly in $Bat3^{-/-}$ testes at P42 (Fig. 1, R–V). These data further support that spermatogenesis is impaired in the absence of *Bat3*.

To gain mechanistic insight into the defect in $Bat3^{-/-}$ spermatocytes, we examined the behavior of meiotic chromosome cores. Using an antibody against SYCP3, we noticed that synapsis did occur in the absence of $Bat3^{-/-}$; however, a higher number of unsynapsed or partially synapsed chromosomes were observed (Fig. 2 E and Fig. S1, B and C; available at http://www.jcb.org/cgi/content/full/jcb.200802113/DC1) relative to normal controls (Fig. 2 A and Fig. S1 A). Consistent with these morphological abnormalities, multiple γ-H2AX–positive foci were observed on paired and unpaired $Bat3^{-/-}$ chromosomes (Fig. 2 F and Fig. S1, E and F). The paired regions heavily coated with γ-H2AX (Fig. S1 F) suggest the existence of nonhomologously paired regions in $Bat3^{-/-}$ chromosomes. In contrast, only the partially paired XY was positive for γ-H2AX staining in $Bat3^{+/+}$ samples (Fig. 2 B and Fig. S1 D). We also detected abnormal SYCP3 and γ-H2AX staining in $Bat3^{-/-}$ cryosections (Fig. 2, O–T). These data indicate that multiple synaptic abnormalities occur in $Bat3^{-/-}$ pachytene spermatocytes.

Next, we analyzed the localization of the early recombination repair marker Rad51. Rad51 was located along synapsed and asynapsed portions of SCs in $Bat3^{+/+}$ zygotene spermatocytes and gradually disappeared in late zygotene/early pachytene (Fig. 2 C). In contrast, $Bat3^{-/-}$ pachytene spermatocytes retained a significant number of Rad51 foci (Fig. 2 G) even though the number and localization of Rad51 recombinase complexes appeared normal in meiotic nuclei during early prophase (not depicted). We also stained for replication protein A (RPA), which colocalizes with Rad51 (Sigurdsson et al., 2001; Govin et al., 2006). We detected a significant number of RPA foci in $Bat3^{-/-}$ (Fig. 2 H) but only trace levels in $Bat3^{+/+}$ (Fig. 2 D) pachytene spermatocytes. These findings suggest that *Bat3* is required for proper chromosomal pairing, recombination, and desynapsis.

Although most spermatocytes in $Bat3^{-/-}$ mice arrested and died in meiotic prophase I, we observed a small number of spermatids and sperm cells in chromosome spread preparations (Fig. 2 J). These elongated spermatids and sperm heads showed abnormal shape and mislocalization of TP-1 (Fig. 2, K–N). TP-1 functions in histone replacement within the sperm head (Sassone-Corsi, 2002). Thus, Bat3 may regulate histone replacement in postmeiotic GCs.

The phenotype observed in $Bat3^{-/-}$ males is characterized by the failure of SCs to disassemble, resulting in differentiation

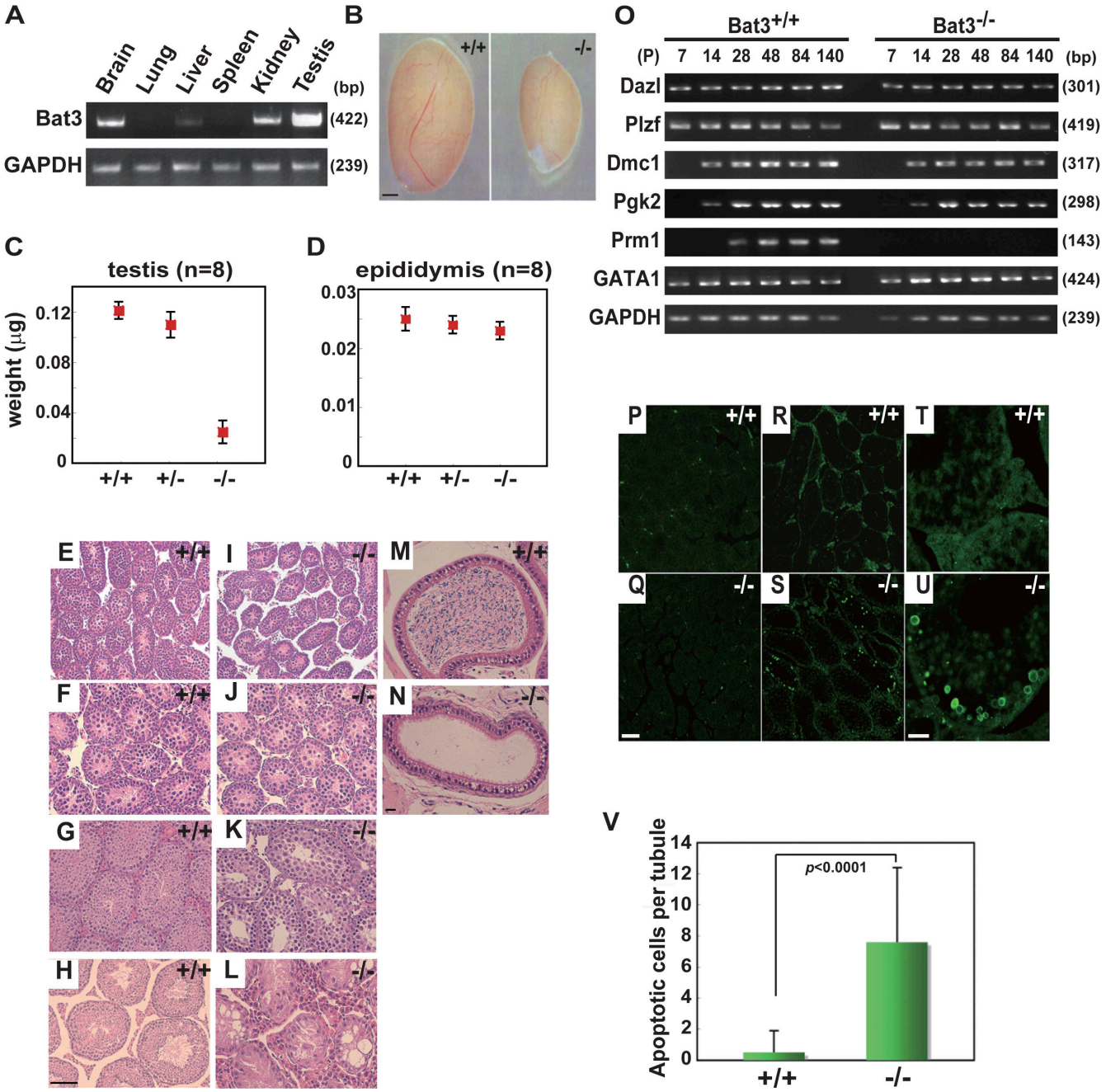

Figure 1. **Developmental defects and increased apoptosis in *Bat3*$^{-/-}$ male GCs.** (A) High expression of Bat3 in testis. Representative Bat3 expression in the indicated organs of P42 *Bat3*$^{+/+}$ male mice was examined by semiquantitative RT-PCR. GAPDH (glyceraldehyde-3-phosphate dehydrogenase), loading control. (B–D) Phenotypes in *Bat3*$^{+/+}$ and *Bat3*$^{-/-}$ testis and epididymis. Testes and epididymides were prepared from P120 *Bat3*$^{+/+}$, *Bat3*$^{+/-}$, and *Bat3*$^{-/-}$ male littermates. The size (B) and weight of testes (C) and epididymides (D) were measured (n = 8). Error bars represent SD. (E–L) Representative histological sections of hematoxylin and eosin–stained P7 (E and I), P14 (F and J), P42 (G and K), and P140 (H and L) testes and P140 epididymides (M and N). (O) Stage-specific expression of the indicated genes during spermatogenesis was analyzed by semiquantitative RT-PCR. GAPDH, loading control. Samples were prepared at the indicated developmental stages (P, postnatal day). (P–V) Increase in the number of TUNEL-positive *Bat3*$^{-/-}$ male GCs. Testis sections from P7 (P and Q) and P42 (R and S, low magnification; T and U, high magnification) of *Bat3*$^{+/+}$ and *Bat3*$^{-/-}$ are shown. TUNEL-positive cells were counted on P42 *Bat3*$^{+/+}$ and *Bat3*$^{-/-}$ sections (V). Bar graph represents mean ± SD (error bars; n = 20). Statistical significance was assessed using the unpaired t test. Bars: (B) 1 mm; (H and Q) 100 μm; (N and U) 20 μm.

arrest and apoptosis of spermatocytes, essentially leading to male infertility. Interestingly, this phenotype is similar to that seen in *Hsp70-2*$^{-/-}$ male mice (Dix et al., 1996). Hsp70-2 has also been found to regulate TP-1 and -2 (Govin et al., 2006). In addition, Bat3 has been shown to bind Hsp70/Hsc70 in a BAG domain–dependent manner and inhibits Hsp70-mediated protein refolding in vitro (Thress et al., 2001). Such mounting evidence prompted us to investigate a functional interaction between Hsp70-2 and Bat3.

Hsp70-2 was abundantly expressed in spermatocytes and round spermatids but not spermatogonia in *Bat3*$^{+/+}$ mice (Fig. 3, A and C). In contrast, Hsp70-2 was undetectable in *Bat3*$^{-/-}$

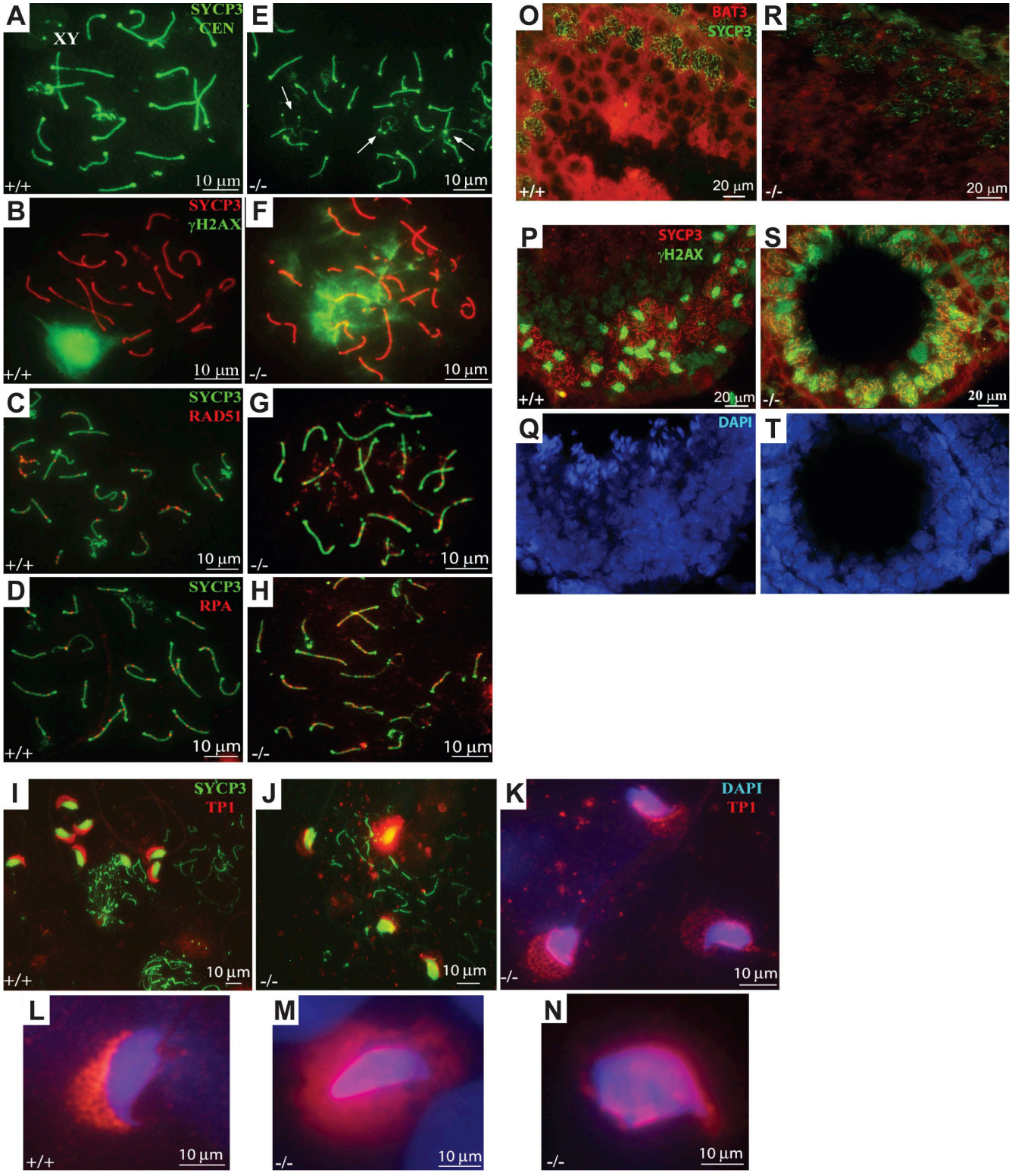

Figure 2. **Bat3 is required for SC formation.** (A–N) Spermatocyte surface spreads were prepared from *Bat3*$^{+/+}$ and *Bat3*$^{-/-}$ testes. SCs were visualized with SYCP3 antibody, and centromeres were stained with CEN antibodies (A and E). Analysis of SYCP3/γ-H2AX (B and F), SYCP3/Rad51 (C and G), SYCP3/RPA (D and H), SYCP3/TP1 (I and J), and TP1/DAPI (K–N). Arrows indicate abnormal SC formation in *Bat3*$^{-/-}$ samples (E). (O–T) Frozen sections from *Bat3*$^{+/+}$ and *Bat3*$^{-/-}$ testes were stained with Bat3/SYCP3 (O and R) and SYCP3/γ-H2AX (P and S) antibodies. DNA was stained with DAPI (Q and T).

mice (Fig. 3, B and D). To eliminate the possibility that abnormal Hsp70-2 protein levels in *Bat3*$^{-/-}$ mice resulted from the loss of GCs at later developmental stages, we analyzed sections prepared at earlier stages. At P7, Hsp70-2 was not detected in either *Bat3*$^{+/+}$ or *Bat3*$^{-/-}$ mice (Fig. 3, K and L). In contrast, Hsp70-2 became evident at P14 in *Bat3*$^{+/+}$ but not *Bat3*$^{-/-}$ mice

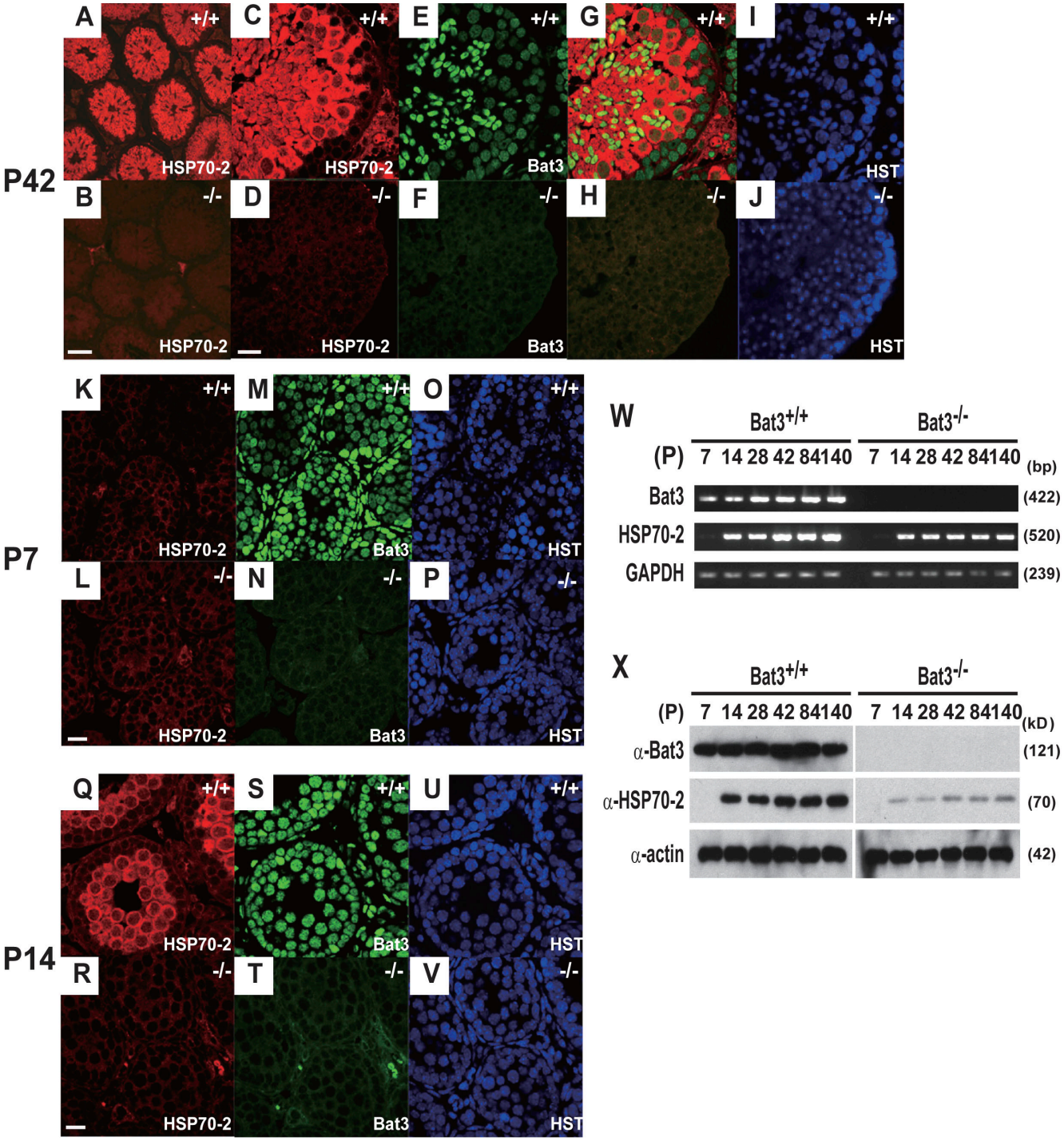

Figure 3. **Decreased Hsp70-2 protein levels in *Bat3*$^{-/-}$ male GCs.** (A–J) P42 *Bat3*$^{+/+}$ and *Bat3*$^{-/-}$ testis sections were stained with Hsp70-2 (A–D) and Bat3 (E and F) antibodies. Hoechst33258 for DNA staining (I and J). Merged images (G and H). (K–V) Defective accumulation of Hsp70-2 at an early stage of spermatogenesis. P7 (K–P) and P14 (Q–V) *Bat3*$^{+/+}$ and *Bat3*$^{-/-}$ testis sections were stained using Hsp70-2 (K, L, Q, and R) and Bat3 (M, N, S, and T) antibodies. DNA was stained by Hoechst 33258 (O, P, U, and V). (W and X) Bat3 and Hsp70-2 mRNA (W) and protein (X) levels in *Bat3*$^{+/+}$ and *Bat3*$^{-/-}$ male GCs were examined at the indicated developmental stages. Bars: (B) 100 μm; (D, L, and R) 20 μm.

(Fig. 3, Q and R). Nuclear staining indicated the presence of GCs in all of the *Bat3*$^{-/-}$ seminiferous tubules (Fig. 3 V).

We next investigated Hsp70-2 mRNA levels in *Bat3*$^{+/+}$ and *Bat3*$^{-/-}$ testes. In *Bat3*$^{+/+}$ testes, Hsp70-2 became expressed at P14, and Bat3 expression occurred at P7 (Fig. 3 W). Interestingly, Hsp70-2 transcript levels were not significantly affected (Fig. 3 W), but Hsp70-2 protein levels were significantly lower in *Bat3*$^{-/-}$ GCs (Fig. 3 X). Therefore, we speculated that *Bat3* deficiency might accelerate Hsp70-2 protein degradation.

We first examined whether *Bat3* knockout or knockdown (KD) could reduce Hsp70-2 protein levels. Hsp70-2 levels were

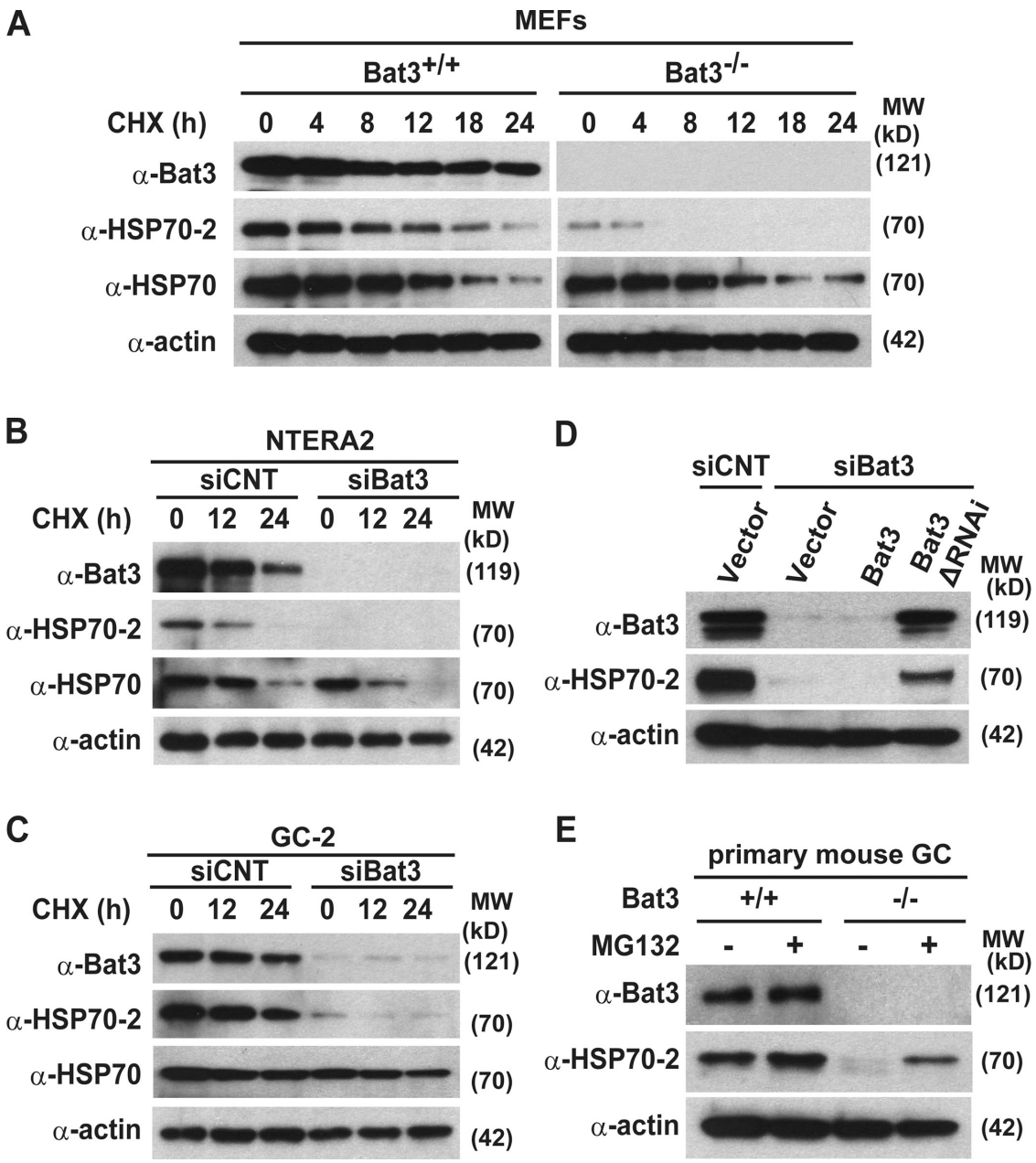

Figure 4. **Bat3 is required for Hsp70-2 protein stability in multiple tissues.** (A–C) Bat3, Hsp70-2, and Hsp70 protein levels were evaluated in *Bat3*$^{+/+}$ and *Bat3*$^{-/-}$ MEFs (A), a human teratocarcinoma cell line, NTERA2 (B), and a mouse spermatocyte cell line, GC-2 (C), in the presence or absence of Bat3 with cycloheximide treatment for the indicated times (in hours). (D) Decreased Hsp70-2 protein stability induced by Bat3 KD was rescued by the RNAi-resistant Bat3 mutant (Bat3ΔRNAi). siCNT, control siRNA. (E) Hsp70-2 levels in primary *Bat3*-deficient male GCs were restored by proteasome inhibitor (MG132) treatment.

significantly lower in both *Bat3*$^{-/-}$ MEFs (Fig. 4 A) and multiple cell lines depleted for Bat3 (Fig. 4, B and C). We excluded potential off-target effects by introducing a Bat3 mutant resistant to RNAi (ΔRNAi-B3; Fig. 4 D; Sasaki et al., 2007). These data demonstrate that Bat3 is required for maintaining Hsp70-2 protein levels. We also found that Hsp70-2 protein levels were restored in *Bat3*$^{-/-}$ mouse primary GCs after treatment with MG132 (Fig. 4 E). Because Bat3 regulates the chaperone function of Hsp70 in vitro (Thress et al., 2001), we also examined Hsp70 protein levels. Notably, we found that Hsp70 protein levels were not significantly affected by Bat3 status (Fig. 4, A–C).

We then examined whether Bat3 binds Hsp70-2. We transfected Flag–Hsp70-2 plus Myc-tagged full-length or deletion mutants of Bat3 into HEK293T cells (Fig. 5 A). Immunoprecipitation assays showed that Bat3 interacts with Hsp70-2 (Fig. 5 B) and that the BAG domain is essential for this interaction (Fig. 5 C), as shown previously for other members of the HSP70 family of proteins (Thress et al., 2001).

Next, we tested whether Bat3 KD could induce Hsp70-2 poly-Ub. We transfected U2OS cells with control or Bat3-targeted RNAi in combination with Flag–Hsp70-2 and HA-ubiquitin. Bat3 KD significantly increased the level of polyubiquitylated Hsp70-2 (Fig. 5 D). Hsp70-2 was also highly ubiquitylated in

Bat3$^{-/-}$ GCs (Fig. 5 E), suggesting that Bat3 negatively regulates the poly-Ub and subsequent degradation of Hsp70-2.

Because Hsp70 stability was not affected by Bat3 loss (Fig. 4, A–C), we speculated that the offending lysine (Lys) residues targeted by poly-Ub are specific to Hsp70-2. We aligned the amino acid sequences of Hsp70 and Hsp70-2 and identified unique Lys residues in Hsp70-2 (Fig. 5 F). We created a series of deletion mutants to exclude Lys residues in Hsp70-2 (Fig. 5 G). Only the ΔN196 mutant lacking amino acids 1–196 could not be polyubiquitylated (Fig. 5 H). Further mutational analysis of Hsp70-2 identified Lys residues critical for poly-Ub (Fig. 5 I). These residues are conserved between human and mice (unpublished data). These data indicate that Bat3 binds and stabilizes Hsp70-2. Here, we propose a model in which the Bat3–Hsp70-2 interaction protects Hsp70-2 from ubiquitin ligase (Fig. 5 J).

We examined the expression of Bat3 and Hsp70-2 in Leydig and Sertoli cells. Hsp70-2 transcripts were undetectable in either cell type, whereas Bat3 transcripts were detectable in both (Fig. S2, available at http://www.jcb.org/cgi/content/full/jcb.200802113/DC1). The absence of Hsp70-2 in both cells was confirmed by immunostaining (Fig. S3). In addition, no significant differences in the staining pattern of calretinin (a Leydig cell marker) and Gata4 (a Sertoli cell marker) were observed in the absence of Bat3 (Fig. S3). These findings further support the idea that the GC phenotypes in *Bat3*$^{-/-}$ mice were caused by intrinsic defects.

Bat3 contains an N-terminal ubiquitin-like domain that inhibits the protein refolding activity of Hsc70/Hsp70 in vitro (Thress et al., 2001). These findings implicate Bat3 in the regulation of molecular chaperones. However, the in vivo targets of Bat3 were previously unknown. In this study, we have provided the first biochemical and genetic evidence that Bat3 stabilizes Hsp70-2 by inhibiting its poly-Ub. Importantly, this interaction is also crucial for Hsp70-2 function in spermatogenesis.

In the BAG family of proteins, Bag-1 has been shown to act as a cochaperone and stimulate CHIP (C terminus of Hsp70-interacting protein)-mediated degradation of the glucocorticoid hormone receptor (Demand et al., 2001). Bag-1 recruits Hsc70 complexes to the proteasome and stimulates the proteasomal degradation of target proteins (Briknarova et al., 2001). Another BAG family member, Bag-2, acts as an inhibitor of the CHIP ubiquitin ligase (Arndt et al., 2005; Dai et al., 2005). In addition, Hsp70-2 is up-regulated in certain human cancers and is required for cancer cell growth and survival (Rohde et al., 2005; Daugaard et al., 2007). Therefore, it is tempting to speculate that Bat3 and Hsp70-2 cooperate to regulate diverse chaperone-assisted processes in both healthy and diseased cells. The identification of Bat3 as a critical regulator of chromosome dynamics during meiosis suggests that other BAG family proteins might play similar roles in maintaining chromosome integrity.

Homologues of Hsp70-2 and Bat3 are present in male GCs of many animals, suggesting that the requirement for Bat3–Hsp70-2 chaperone function in spermatogenic cells is conserved. An estimated 15% of couples worldwide remain childless because of infertility (de Kretser, 1997); however, little is know about the genetic causes of human infertility. Based on our study, future studies should investigate whether mutations or polymorphisms in Bat3 underlie idiopathic male infertility.

Materials and methods

Histological analysis

For immunohistochemistry, paraffin-embedded sections were deparaffinized and rehydrated followed by antigen retrieval in boiled 10-mM sodium citrate buffer. Sections were blocked in 10% normal goat serum in PBS for 1 h at room temperature and incubated with primary antibody at 4°C overnight. After washing in PBS/0.3% Triton X-100 three times, the sections were incubated with secondary antibody for 1 h at room temperature. The sections were washed three times and mounted in ProLong Gold Antifade Reagent (Invitrogen). TUNEL staining was performed using an In Situ Cell Death Detection kit (Roche) according to the manufacturer's protocol. Primary antibodies used were polyclonal anti–mouse Bat3 antibody (Sasaki et al., 2007), Hsp70-2/HspA2 (M06; Abnova Corp.), calretinin (Santa Cruz Biotechnology, Inc.), and Gata-4 (Santa Cruz Biotechnology, Inc.). Secondary antibodies used were goat anti–rabbit AlexaFluor488 and goat anti–mouse AlexaFluor594 (Invitrogen). Hoechst33258 (Invitrogen) was used to visualize nuclei. Confocal images were acquired on a confocal microscope (LSM510; Carl Zeiss, Inc.) using 10×/0.5 NA, 20×/0.75 NA, and 63×/1.2 NA water immersion objectives. Three fluorophores (Hoechst33258, AlexaFluor488, and AlexaFluor594) were imaged sequentially using 351-, 488-, and 543-nm laser excitation and appropriate bandpass emission filters. LSM Image Browser (Carl Zeiss, Inc.) was used for capturing and overlaying images of different colors, and Photoshop CS2 (Adobe) was used to crop the images to proper size.

Immunostaining of surface-spread spermatocytes

Staining was performed as previously described (Dobson et al., 1994). The developmental stages of male GCs were determined based on the morphology and appearance of the XY bivalent and the localization of meiotic markers Rad51 and RPA. Chromosome cores and SCs were visualized using antibodies against SYCP3 and SYCP1 proteins (Dobson et al., 1994). RPA (provided by J. Ingles, University of Toronto, Toronto, Canada) and RAD51/DMC1 antibodies were previously described (Moens et al., 2002). Centromeres were visualized with human CREST serum (provided by S. Varmuza, University of Toronto, Toronto, Canada). TP-1 antibody was a gift from S. Kistler (University of South Carolina, Columbia, SC). γ-H2AX antibody was obtained from Abcam. ProLong Gold Antifade reagent (Invitrogen) was used as a mounting agent to prevent fading of fluorescent signal. Rhodamine and FITC fluorochromes were used to visualize antibody-bound proteins, whereas DAPI fluorochrome allowed visualization of DNA. The images were acquired on a Polyvar microscope (model 602601; Carl Zeiss, Inc.) with oil immersion fluorescent objective lenses (Carl Zeiss, Inc.) of 40×/1 NA and 100×/1.32 NA magnification and were recorded with a cooled digital color camera (DP70; Olympus) using Image Pro 4.0 software (Media Cybernetics, Inc.). For image processing, Photoshop 7.0 was used. Using Photoshop, the brightness and contrast were enhanced, and the two images of different colors were overlapped and cropped to proper size.

RT-PCR

Sertoli and Leydig cells were isolated from three wild-type mice as previously described (Anway et al., 2003). Total RNA was extracted from the cells and testes using TRIZOL (Invitrogen). First-strand cDNA was synthesized using a SuperScript First-Strand kit (Invitrogen) according to the manufacturer's instructions. Gene-specific primers are listed in Table S2 (available at http://www.jcb.org/cgi/content/full/jcb.200802113/DC1).

Cell lines, transfections, and RNAi

U2OS, 293T, NTERA2, and GC-2 cells were obtained from the American Type Culture Collection. Synthetic siRNA oligoduplexes for Bat3 as previously described (Sasaki et al., 2007) were purchased from Dharmacon. Cells were cultured to 60% confluency in Opti-MEM medium (Invitrogen) and transfected with siRNA oligoduplexes (40-nM final concentration) plus 3 μl Lipofectamine 2000 (Invitrogen). At 6–8 h after transfection, the medium was changed to complete medium. Transfected cells were assayed 48 h after transfection unless otherwise indicated. All control samples were transfected with control siRNA oligoduplex (Dharmacon).

Western blot analysis

Protein samples were prepared in lysis buffer (0.1% SDS, 0.1% sodium deoxycholate, 1% Triton X-100, 20 mM Tris-HCl, pH 7.5, 150 mM NaCl,

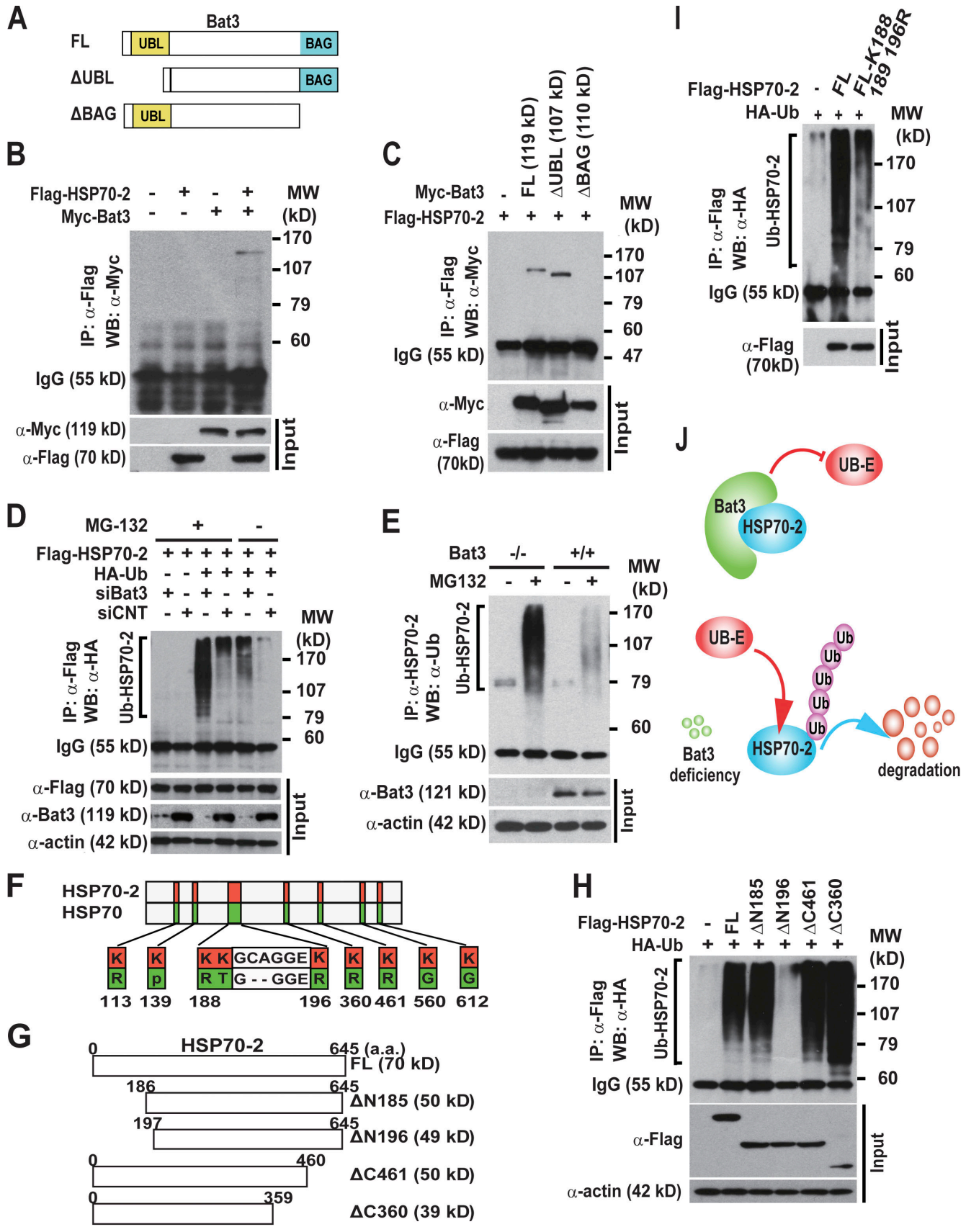

Figure 5. **Bat3 binds and negatively regulates the poly-Ub of Hsp70-2.** (A–C) The Bat3 BAG domain is required for interaction with Hsp70-2. 293T cells were transfected with Flag–Hsp70-2 and a series of Myc-Bat3 deletion mutants (A). Lysates were immunoprecipitated with anti-Flag antibody and immunoblotted with anti-Myc antibody (B and C). (D) Negative regulation of Hsp70-2 poly-Ub by Bat3. Flag–Hsp70-2 and HA-Ub plus either siBat3 or siCNT (control siRNA) were transfected into U2OS cells. The lysates were immunoprecipitated and immunoblotted with anti-HA antibody. (E) Increased poly-Ub

1 mM EDTA, 10 mM NaF, and protease inhibitor cocktail [Roche]). 20 µg of lysates was immunoblotted according to standard procedures. Proteins were transferred to an Immobilon-P membrane (Millipore). Blots were incubated with the primary antibody at 4°C overnight and with a horseradish peroxidase–conjugated secondary antibody at room temperature for 1 h. Signals were detected using Enhanced Chemiluminescence reagents (GE Healthcare). Primary antibodies used were as follows: anti–mouse (Sasaki et al., 2007) and anti–human Bat3 (a gift from S. Kornbluth, Duke University, Durham, NC); anti-Hsp70 (K-20) and anti-HA (F-7; Santa Cruz Biotechnology, Inc.); and anti-Flag M2 and anti-actin (Sigma-Aldrich).

Immunoprecipitations

293T cells were transfected with Flag–Hsp70-2 plus pcDNA3 control vector (Invitrogen) or Myc-Bat3. Cells were lysed in buffer (50 mM Tris-HCl, 150 mM NaCl, and 1% NP-40) supplemented with a protease inhibitor cocktail (Roche) for 30 min on ice and cleared by centrifugation. Extracts were incubated with the appropriate antibodies at 4°C for 16 h with rotation and incubated for an additional 2–3 h with protein A/G agarose beads (Santa Cruz Biotechnology, Inc.). Samples were fractionated by SDS-PAGE and subjected to immunoblotting as described in the previous section.

Hormone measurement

Serum levels of testosterone, LH, and FSH were measured in P40 *Bat3*$^{+/+}$ and *Bat3*$^{-/-}$ mice. LH and FSH were measured by the Center for Research in Reproduction Ligand Assay and Analysis Core of the University of Virginia. Testosterone was measured by an ELISA kit according to the manufacturer's protocol (Assay Designs).

Online supplemental material

Fig. S1 shows additional pictures for SYCP3/γ-H2AX staining of SCs. Fig. S2 demonstrates that Hsp70-2 transcripts are undetectable in Leydig and Sertoli cells. Fig. S3 shows that Hsp70-2 protein is also undetectable in Leydig and Sertoli cells. Table S1 shows that *Bat3* deficiency does not affect serum levels of testosterone, LH, or FSH. Table S2 lists RT-PCR primer sets used in this study. Online supplemental material is available at http://www.jcb.org/cgi/content/full/jcb.200802113/DC1.

This paper is dedicated to Peter B. Moens and his outstanding contributions in the field of reproductive cell biology. We sincerely thank Sally Kornbluth for helpful discussion, human Bat3 antibody, and human myc-Bat3 plasmid; Steve Kistler for TP1 antibody; Andrew Wakeham for embryonic stem cell injection; Andrea Jurisicova and Andras Nagy for help in the initial stage of the project; Barbara Spyropoulos for antibody preparation; and Emma Gooding and David Sealey for editing.

H. Okada is supported by a grant from the Canadian Institutes of Health Research (MOP84353). The University of Virginia Center for Research in Reproduction Ligand Assay and Analysis Core is supported by National Institute of Child Health and Human Development/National Institutes of Health (Specialized Cooperative Centers Program in Reproduction and Infertility Research) grant U54-HD28934.

Submitted: 19 February 2008
Accepted: 7 July 2008

References

Allen, J.W., D.J. Dix, B.W. Collins, B.A. Merrick, C. He, J.K. Selkirk, P. Poorman-Allen, M.E. Dresser, and E.M. Eddy. 1996. HSP70-2 is part of the synaptonemal complex in mouse and hamster spermatocytes. *Chromosoma.* 104:414–421.

Anway, M.D., J. Folmer, W.W. Wright, and B.R. Zirkin. 2003. Isolation of sertoli cells from adult rat testes: an approach to ex vivo studies of Sertoli cell function. *Biol. Reprod.* 68:996–1002.

Arndt, V., C. Daniel, W. Nastainczyk, S. Alberti, and J. Hohfeld. 2005. BAG-2 acts as an inhibitor of the chaperone-associated ubiquitin ligase CHIP. *Mol. Biol. Cell.* 16:5891–5900.

Boer, P.H., C.N. Adra, Y.F. Lau, and M.W. McBurney. 1987. The testis-specific phosphoglycerate kinase gene pgk-2 is a recruited retroposon. *Mol. Cell. Biol.* 7:3107–3112.

Bolcun-Filas, E., Y. Costa, R. Speed, M. Taggart, R. Benavente, D.G. De Rooij, and H.J. Cooke. 2007. SYCE2 is required for synaptonemal complex assembly, double strand break repair, and homologous recombination. *J. Cell Biol.* 176:741–747.

Briknarova, K., S. Takayama, L. Brive, M.L. Havert, D.A. Knee, J. Velasco, S. Homma, E. Cabezas, J. Stuart, D.W. Hoyt, et al. 2001. Structural analysis of BAG1 cochaperone and its interactions with Hsc70 heat shock protein. *Nat. Struct. Biol.* 8:349–352.

Buaas, F.W., A.L. Kirsh, M. Sharma, D.J. McLean, J.L. Morris, M.D. Griswold, D.G. de Rooij, and R.E. Braun. 2004. Plzf is required in adult male germ cells for stem cell self-renewal. *Nat. Genet.* 36:647–652.

Costa, Y., and H.J. Cooke. 2007. Dissecting the mammalian synaptonemal complex using targeted mutations. *Chromosome Res.* 15:579–589.

Costa, Y., R. Speed, R. Ollinger, M. Alsheimer, C.A. Semple, P. Gautier, K. Maratou, I. Novak, C. Hoog, R. Benavente, and H.J. Cooke. 2005. Two novel proteins recruited by synaptonemal complex protein 1 (SYCP1) are at the centre of meiosis. *J. Cell Sci.* 118:2755–2762.

Dai, Q., S.B. Qian, H.H. Li, H. McDonough, C. Borchers, D. Huang, S. Takayama, J.M. Younger, H.Y. Ren, D.M. Cyr, and C. Patterson. 2005. Regulation of the cytoplasmic quality control protein degradation pathway by BAG2. *J. Biol. Chem.* 280:38673–38681.

Daugaard, M., T. Kirkegaard-Sorensen, M.S. Ostenfeld, M. Aaboe, M. Hoyer-Hansen, T.F. Orntoft, M. Rohde, and M. Jaattela. 2007. Lens epithelium-derived growth factor is an Hsp70-2 regulated guardian of lysosomal stability in human cancer. *Cancer Res.* 67:2559–2567.

de Kretser, D.M. 1997. Male infertility. *Lancet.* 349:787–790.

Demand, J., S. Alberti, C. Patterson, and J. Hohfeld. 2001. Cooperation of a ubiquitin domain protein and an E3 ubiquitin ligase during chaperone/proteasome coupling. *Curr. Biol.* 11:1569–1577.

Desmots, F., H.R. Russell, Y. Lee, K. Boyd, and P.J. McKinnon. 2005. The reaper-binding protein scythe modulates apoptosis and proliferation during mammalian development. *Mol. Cell. Biol.* 25:10329–10337.

Desmots, F., H.R. Russell, D. Michel, and P.J. McKinnon. 2007. Scythe regulates apoptosis inducing factor stability during endoplasmic reticulum stress induced apoptosis. *J. Biol. Chem.* 283:3264–3271.

Dix, D.J., J.W. Allen, B.W. Collins, C. Mori, N. Nakamura, P. Poorman-Allen, E.H. Goulding, and E.M. Eddy. 1996. Targeted gene disruption of Hsp70-2 results in failed meiosis, germ cell apoptosis, and male infertility. *Proc. Natl. Acad. Sci. USA.* 93:3264–3268.

Dobson, M.J., R.E. Pearlman, A. Karaiskakis, B. Spyropoulos, and P.B. Moens. 1994. Synaptonemal complex proteins: occurrence, epitope mapping and chromosome disjunction. *J. Cell Sci.* 107:2749–2760.

Fawcett, D.W. 1956. The fine structure of chromosomes in the meiotic prophase of vertebrate spermatocytes. *J. Biophys. Biochem. Cytol.* 2:403–406.

Govin, J., C. Caron, E. Escoffier, M. Ferro, L. Kuhn, S. Rousseaux, E.M. Eddy, J. Garin, and S. Khochbin. 2006. Post-meiotic shifts in HSPA2/HSP70.2 chaperone activity during mouse spermatogenesis. *J. Biol. Chem.* 281:37888–37892.

Hamer, G., K. Gell, A. Kouznetsova, I. Novak, R. Benavente, and C. Hoog. 2006. Characterization of a novel meiosis-specific protein within the central element of the synaptonemal complex. *J. Cell Sci.* 119:4025–4032.

Kleene, K.C., R.J. Distel, and N.B. Hecht. 1984. Translational regulation and deadenylation of a protamine mRNA during spermiogenesis in the mouse. *Dev. Biol.* 105:71–79.

of Hsp70-2 in *Bat3*$^{-/-}$ primary male GCs. *Bat3*$^{+/+}$ and *Bat3*$^{-/-}$ GCs were cultured in the presence or absence of proteasome inhibitor (MG132). Protein samples were immunoprecipitated with anti–Hsp70-2 antibody and immunoblotted with anti-Ub antibody. (F–H) Identification of Lys residues required for Hsp70-2 poly-Ub. Schematic representation of lysine residues specific to Hsp70-2 (F) and a series of Flag–Hsp70-2 deletion mutants (G). The deletion mutants and HA-Ub were transfected into HEK293T cells. Protein lysates were immunoprecipitated with anti-Flag antibody and immunoblotted with anti-HA antibody (H). (I) Significant reduction in Hsp70-2 poly-Ub by introducing point mutations. N-terminal Hsp70-2 Lys residues were replaced with Arg (K188,189,196R). Flag–Hsp70-2–K188,189,196R and HA-Ub were transfected into HEK293T cells. Protein samples were immunoprecipitated with anti-Flag antibody and immunoblotted with anti-Ub antibody. Input represents the protein levels in the original extracts as determined by conventional Western blotting. (J) A model of Bat3-mediated Hsp70-2 regulation. Bat3 binds Hsp70-2 and may protect Hsp70-2 from the access of ubiquitin ligases (Ub-E). *Bat3* deficiency renders Hsp70-2 susceptible to poly-Ub and subsequent degradation.

Maratou, K., T. Forster, Y. Costa, M. Taggart, R.M. Speed, J. Ireland, P. Teague, D. Roy, and H.J. Cooke. 2004. Expression profiling of the developing testis in wild-type and Dazl knockout mice. *Mol. Reprod. Dev.* 67:26–54.

Moens, P.B. 1994. Molecular perspectives of chromosome pairing at meiosis. *Bioessays.* 16:101–106.

Moens, P.B., N.K. Kolas, M. Tarsounas, E. Marcon, P.E. Cohen, and B. Spyropoulos. 2002. The time course and chromosomal localization of recombination-related proteins at meiosis in the mouse are compatible with models that can resolve the early DNA-DNA interactions without reciprocal recombination. *J. Cell Sci.* 115:1611–1622.

Moses, M.J. 1956. Chromosomal structures in crayfish spermatocytes. *J. Biophys. Biochem. Cytol.* 2:215–218.

Moses, M.J. 1969. Structure and function of the synaptonemal complex. *Genetics.* 61:41–51.

Pogge von Strandmann, E., V.R. Simhadri, B. von Tresckow, S. Sasse, K.S. Reiners, H.P. Hansen, A. Rothe, B. Boll, V.L. Simhadri, P. Borchmann, et al. 2007. Human leukocyte antigen-B-associated transcript 3 is released from tumor cells and engages the NKp30 receptor on natural killer cells. *Immunity.* 27:965–974.

Rohde, M., M. Daugaard, M.H. Jensen, K. Helin, J. Nylandsted, and M. Jaattela. 2005. Members of the heat-shock protein 70 family promote cancer cell growth by distinct mechanisms. *Genes Dev.* 19:570–582.

Sasaki, T., E.C. Gan, A. Wakeham, S. Kornbluth, T.W. Mak, and H. Okada. 2007. HLA-B-associated transcript 3 (Bat3)/Scythe is essential for p300-mediated acetylation of p53. *Genes Dev.* 21:848–861.

Sassone-Corsi, P. 2002. Unique chromatin remodeling and transcriptional regulation in spermatogenesis. *Science.* 296:2176–2178.

Schrans-Stassen, B.H., P.T. Saunders, H.J. Cooke, and D.G. de Rooij. 2001. Nature of the spermatogenic arrest in Dazl−/− mice. *Biol. Reprod.* 65:771–776.

Sigurdsson, S., K. Trujillo, B. Song, S. Stratton, and P. Sung. 2001. Basis for avid homologous DNA strand exchange by human Rad51 and RPA. *J. Biol. Chem.* 276:8798–8806.

Thress, K., W. Henzel, W. Shillinglaw, and S. Kornbluth. 1998. Scythe: a novel reaper-binding apoptotic regulator. *EMBO J.* 17:6135–6143.

Thress, K., E.K. Evans, and S. Kornbluth. 1999a. Reaper-induced dissociation of a Scythe-sequestered cytochrome c-releasing activity. *EMBO J.* 18:5486–5493.

Thress, K., S. Kornbluth, and J.J. Smith. 1999b. Mitochondria at the crossroad of apoptotic cell death. *J. Bioenerg. Biomembr.* 31:321–326.

Thress, K., J. Song, R.I. Morimoto, and S. Kornbluth. 2001. Reversible inhibition of Hsp70 chaperone function by Scythe and Reaper. *EMBO J.* 20:1033–1041.

Toure, A., E.J. Clemente, P. Ellis, S.K. Mahadevaiah, O.A. Ojarikre, P.A. Ball, L. Reynard, K.L. Loveland, P.S. Burgoyne, and N.A. Affara. 2005. Identification of novel Y chromosome encoded transcripts by testis transcriptome analysis of mice with deletions of the Y chromosome long arm. *Genome Biol.* 6:R102.

Wang, P.J., J.R. McCarrey, F. Yang, and D.C. Page. 2001. An abundance of X-linked genes expressed in spermatogonia. *Nat. Genet.* 27:422–426.

Wang, R., and C.C. Liew. 1994. The human BAT3 ortholog in rodents is predominantly and developmentally expressed in testis. *Mol. Cell. Biochem.* 136:49–57.

Zickler, D., and N. Kleckner. 1999. Meiotic chromosomes: integrating structure and function. *Annu. Rev. Genet.* 33:603–754.